High Resolution FTIR Spectrum of Chlorofluoroethyne, FCCCl, below 1000 cm^{-1}. Analysis of the ν_3, ν_4, ν_5, $2\nu_4$, $\nu_4 + \nu_5$ and $2\nu_5$ Bands, and *ab initio* Calculations

J. Breidung, H. Bürger[a], M. Senzlober[a], and W. Thiel
Organisch-chemisches Institut, Universität Zürich, CH-8057 Zürich, Switzerland
[a] Anorganische Chemie, FB 9, Universität-GH Wuppertal, Gaußstr. 20, D-42097 Wuppertal

Z. Naturforsch. **54 a,** 236–244 (1999); received December 2, 1998

High resolution infrared spectra of FCCCl have been measured and analyzed by polynomial methods. In the region below 350 cm^{-1}, the analysis is straightforward and yields parameters for the $v_4 = 1$ and $v_5 = 1$ states. Between 350 and 800 cm^{-1} there are strong anharmonic interactions in the $2\nu_5/\nu_4 + \nu_5/\nu_3/2\nu_4$ tetrad which have been unravelled with the use of a model that employs *ab initio* interaction constants. Observed and theoretically predicted wavenumbers are in excellent agreement for all bands studied.

Key words: Infrared Spectrum; High Resolution; Alkyne; Fermi Resonance; *ab initio* Calculations.

I. Introduction

Dihalogenoethynes XC≡CY (X, Y = F, Cl, Br, and I) are highly reactive molecules. The fluoroethynes FC≡CY in particular have only been synthesized in the recent past. They have been characterized by rotational and rovibrational spectroscopy [1 - 4], and ground state as well as some excited state molecular parameters have been deduced. *Ab initio* calculations at different levels have provided accurate geometries and a reliable picture of the potential function of FCCF [5], FCCCl [6] and FCCBr [7]. These calculations have guided and efficiently assisted the experimental rovibrational studies [1, 6, 7].

We have recently outlined how the interplay of theoretical and experimental studies can provide important and indispensable information which the experiment is unable to furnish by itself. FC≡CCl is a particularly rewarding example for the interaction between theory and experiment [8]. In a previous contribution [6] we have shown how the formerly observed two Σ^+ overtone / combination bands $2\nu_4$ (664.619 cm^{-1} for ^{35}Cl) and $\nu_4 + \nu_5$ (531.490 cm^{-1}) can be interpreted with the help of an anharmonic force field. There are, however, many more rovibrational levels located < 1000 cm^{-1} than those two previously probed. We have therefore optimized our experimental efforts in order to directly observe the three fundamentals $\nu_3(\Sigma^+)$, $\nu_4(\Pi)$ and $\nu_5(\Pi)$. This goal has now been achieved, and furthermore the $2\nu_5(\Sigma^+)$ overtone has been detected both for ^{35}Cl and ^{37}Cl isotopomers. Numerous accompanying hot bands reaching multiply excited levels have been observed as well.

The present paper reports these high resolution infrared spectra and their analysis by the $J(J + 1)$ polynomial method. The experimental data are combined with theoretically predicted interaction constants to develop a physically meaningful interaction model that describes the energy levels of FCCCl up to 1000 cm^{-1}. Some of the results and conclusions have been summarized in a recent review [8] which, however, does not contain detailed spectroscopic or theoretical data.

II. Experimental Details

Fluorochloroethyne has been known since 1970 when its synthesis by HCl elimination from CHF=CCl$_2$ was first reported [9]. IR absorption bands corresponding to the CC and CF stretching vibrations were observed in low-resolution spectra both in the gas phase [9] and in an argon matrix at 10 K [10]. We have prepared FCCCl by thermolysis of 1,3,2-difluorochloro-4,5,6-triazine at 700 °C and purified it

---

Reprint requests to Prof. H. Bürger; Fax: +49 202 439 2901, E-mail: buerger1@uni-wuppertal.de.

0932–0784 / 99 / 0300–0236 $ 06.00 © Verlag der Zeitschrift für Naturforschung, Tübingen · www.znaturforsch.com

Table 1. Experimental details.

	Region (cm^{-1})	Band	Beamsplitter	Detector	Resolution 1/MOP[a] (10^{-3} cm^{-1})	Path length (mm)	Windows	p/T (mbar/°C)	No. of Scans	Signal:Noise Ratio
(1)	80 - 350	ν_5, ν_4	6μm Mylar	Si Bolometer	5.5	1500	PE	6 / 20	140	50
(2)	400 - 750	$2\nu_5, \nu_3$	3.5μm Mylar	CuGe	4.4	1200	KBr	2 / −15	50	100
(3)	360 - 840	$\nu_4 + \nu_5, 2\nu_4$	3.5μm Mylar	CuGe	3.4	280	KBr	6 / 20	112	100

[a] MOPD = maximum optical path difference.

by repeated fractional condensation in vacuo using a −152 °C trap to hold back accompanying FCN [6]. FCCCl is stable at −196 °C and at room temperature at pressures not exceeding 5 mbar.

We have recorded several high resolution FTIR spectra using a Bruker 120 HR interferometer, choosing a resolution ranging from 3.4 to 5.5 × 10^{-3} cm^{-1}. Glass cells of different lengths were employed, and a set-up similar to that described in [11] with an external cell enabling cooling. A path length of 1500 mm was used.

Details concerning the optimized spectra that were finally evaluated are given in Table 1. Calibration was done with H_2O lines in the 150 - 250 and 500 - 600 cm^{-1} regions [12]. The estimated wavenumber accuracy is better than 1 × 10^{-3} cm^{-1}. An interactive Loomis-Wood program was used [13] for the band analysis using ground and $v_5 = 1$ and $v_4 = 1$ lower state parameters as reported [6]. A multi-purpose fit program [14] for the polynomial and the excited state anharmonic resonance models was used.

III. Rovibrational Analysis

All vibrational bands < 1000 cm^{-1} are weak. As predicted [6], the intensities of the ν_4 and ν_5 bands are about two orders of magnitude smaller than those of ν_2 (CF stretch).

Four Σ^+ type parallel bands centered (^{35}Cl) at 416.841 ($2\nu_5$), 531.490 ($\nu_4 + \nu_5$), 574.275 (ν_3) and 664.619 cm^{-1} ($2\nu_4$) were observed in the 350 - 800 cm^{-1} spectral region. The "cold" components of the two stronger ones ($\nu_4 + \nu_5$ and $2\nu_4$) have been analyzed previously [6]. The two additional bands that we have now detected are much weaker, the intensity of ν_3 being not higher than 0.1% of that of the (still weak) $\nu_4 + \nu_5$ combination band.

The observations may be subdivided in two sections, the two perpendicular Σ^+ - Π fundamentals ν_4 and ν_5 with their attached hot bands, and the four above mentioned parallel Σ^+ - Σ^+ bands.

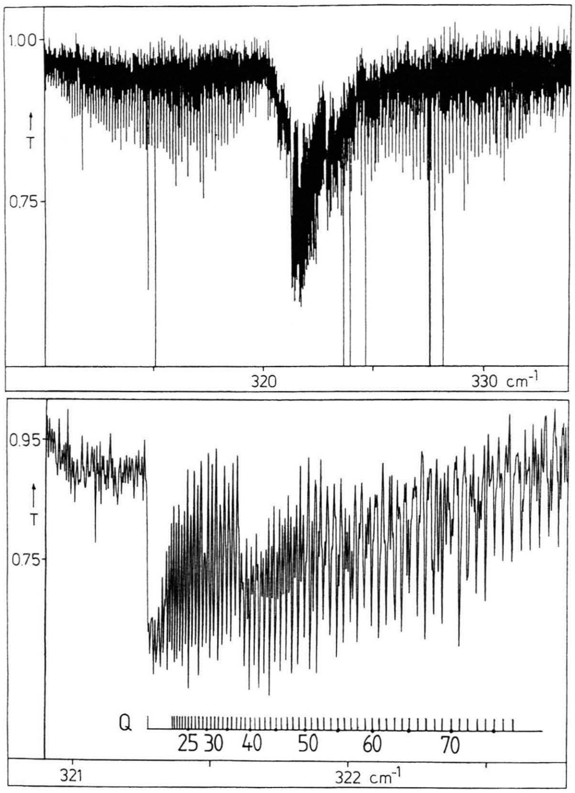

Fig. 1. The ν_4 band of FCCCl. – *Top:* Survey spectrum. The strong, isolated lines standing out are due to residual H_2O in the interferometer. – *Bottom:* Q branch region, with *J* assignment for $FCC^{35}Cl$.

The ν_4 and ν_5 Bands

The two lowest-lying fundamentals ν_4 and ν_5 are Σ^+ - $\Pi_{e,f}$ perpendicular bands with P, Q, R structure. They are centered (^{35}Cl) at 321.27 and 210.50 cm^{-1}. The Q branches are *J*-degraded to higher wavenumbers and consist of several components. First, there are the ^{35}Cl and ^{37}Cl isotopic species in 3 : 1 abundance. Second, there are hot bands, predominantly with ν_4 and ν_5, with Boltzmann factors at room temperature of 0.21 and 0.37, respectively.

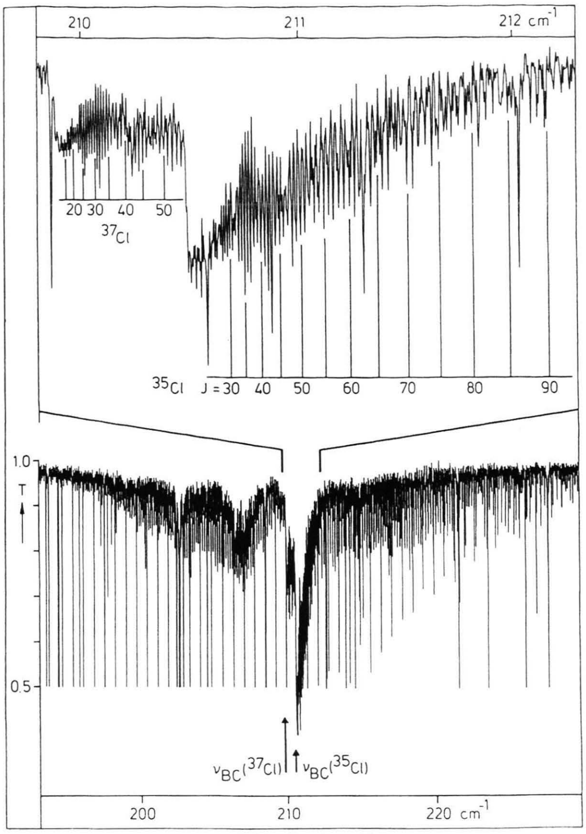

Fig. 2. The ν_5 band of FCCCl. – *Bottom:* Survey spectrum, with band centers indicated. The strong and regular lines cut for clarity at $T = 0.5$ belong either to H_2O or to HNCO [16], which is a hydrolysis product of residual FCN. – *Top:* Detail of the Q branch, with J assignments given for FCC^{35}Cl and FCC^{37}Cl.

The ν_4 and ν_5 bands are illustrated in Figs. 1 and 2, and some line assignments and band centers are quoted. Since ν_4 is closer to the detector's cut-off (near 360 cm^{-1}), the spectrum is noisier than in the ν_5 region, and only the strongest band 010, 1*ef* - 000; notation henceforth $v_3v_4v_5$, ℓ, of the ^{35}Cl species was identified. The ν_4 Q branch of the ^{37}Cl species should be shifted from ^{35}Cl to small wavenumber by $\Delta\nu_4 = (\Delta\nu_{4+5} - \Delta\nu_5) = 0.24$ cm^{-1}. In fact a Q branch edge is visible, Fig. 1, but only a limited number of lines belonging to the P branch could be assigned.

In the ν_5 band altogether five band systems have been assigned. Both the Q and P, R branches of the dominating ^{35}Cl cold band could be followed up to $J \approx 90$. The corresponding Q branch of the ^{37}Cl species was resolved and visible up to $J = 54$, beyond which it is hidden by the stronger ^{35}Cl features. P and R lines were assigned up to $J = 90$.

The most prominent hot bands 002, 0*e* - 001, 1*ef* and 002, 2*ef* - 001, 1*ef* of the ^{35}Cl species are centered at 206.34 and 210.50 cm^{-1}, respectively. While the former gives rise to an isolated and well resolved Q branch, Fig. 2, and P and R lines as well, the *e* - *f* and *f* - *e* Q branches of the latter coincide within 0.005 cm^{-1} with that of the cold band and thus were blended. Since however the P and R branch lines occur as *e* - *e* and *f* - *f* doublets we were able to access the 0*e*, 2*e* and 2*f* sublevels of the $v_5 = 2$ vibrational state. This information on the 002, 2*ef* state is particularly valuable for the deperturbation of the Σ^+ tetrad (see below).

Vibrational term energies $G_{v\ell}$ were taken in the usual way:

$$G_{v\ell} = \sum_s \omega_s\left(v_s + \frac{d_s}{2}\right) + \sum_{s\leq s'} x_{ss'}\left(v_s + \frac{d_s}{2}\right)\left(v_{s'} + \frac{d_{s'}}{2}\right) + \sum_{t\leq t'} g_{tt'}^{\ell_t \ell_{t'}} \quad (1)$$

The term value difference $\nu_0 = G_{v'\ell'} - G_{v''\ell''}$ is related to the experimentally determined band center ν_{BC} by

$$\nu_{BC} = \nu_0 - [B'\ell'^2 - B''\ell''^2]. \quad (2)$$

Rotational energies F_{vJ} were taken as

$$F_{vJ} = B_v J(J+1) - D_v[J(J+1)]^2 + H_v[J(J+1)]^3. \quad (3)$$

For states with $\ell \neq 0$ (Π...) two substates *e* and *f* exist. Their energy difference is given by

$$q_v = B_v^f - B_v^e \quad (4)$$

and

$$B_v = \frac{1}{2}(B_v^e + B_v^f). \quad (5)$$

Deperturbation of the ℓ-type resonance was performed using a matrix element

$$\langle v_t = 1, v_{t'} = 1, J, k = 0, |\mathbf{H}/hc| v_t = 1, v_{t'} = 1, J, k \pm 2\rangle$$

$$= W_{tt'}[J(J+1) - k(k \pm 1)]^{1/2} \quad (6)$$

$$\cdot\ [J(J+1) - (k \pm 1)(k \pm 2)]^{1/2}$$

with $k = \ell_t + \ell_{t'}$; $t = 4$ and $t' = 5$, and $t = t' = 5$.

Table 2. Ground state parameters (cm^{-1}) of FCCCl.

	— FCC^{35}Cl —				— FCC^{37}Cl —		
	MMW [2]	GSCD	Combined "best" fit	*ab initio*	MMW [2]	GSCD	Combined "best" fit
$B \times 10^2$	7.421 281 5(19)	7.421 285 4(65)	7.421 280 37(83)	7.383	7.243 892 1(14)	7.243 918(12)	7.243 894 2(13)
$D_J \times 10^9$	4.819 2(86)	4.815 6(51)	4.813 1(25)	4.425 [6] (D_e)	4.593 2(55)	4.623(10)	4.602 4(46)
J'_{max}	40	114	114		41	107	107
No. of data	16	1072	1088		12	390	402
σ(Fit) $\times 10^5$	0.16	21.2	1.0		0.10	24.4	0.8

Table 3. Results of band fits for FCCCl (cm^{-1}).

$v_3v_4v_5, \ell$	ν_{BC}	$(B''\text{-}B')\times 10^4$	$(D''\text{-}D')\times 10^9$	$q'_v \times 10^5$	J'_{max} [a]	No.[a] of data	$\sigma \times 10^4$
FCC^{35}Cl:							
002, 0*e* - 001, 1*ef*	206.339 54(7)	−1.689 9(7)	−0.964(4)		102	125	3.6
002, 2*e* - 001, 1*e*	210.496 70(14)	−2.044 0(9)	0.620(12)		87	85	4.5
002, 2*f* - 001, 1*f*	210.497 39(16)	−1.444 0(10)	−0.098(13)		87	98	4.5
001, 1*ef* - 000	210.502 45(5)	−1.740 3(4)	−0.127(4)	5.915 8(11)	94	220	3.3
010, 1*ef* - 000	321.270 24(6)	−1.968 3(6)	−0.147(7)	3.713 8(16)	82	183	3.5
002, 0*e* - 000	416.841 33(6)	−3.433 2(4)	−1.118(5)		93	139	2.9
012, 1*e* - 001, 1*e*	531.076 80(5)	−3.823 4(4)	0.193(5)		93	143	2.9
012, 1*f* - 001, 1*f*	531.076 27(6)	−3.421 3(33)	−0.501(4)		102	162	3.4
011, 0*e* - 000	531.489 51(6)	−3.591 4(6)	−3.856(17)[b]		101	193	3.4
100 - 000	574.274 63(9)	−0.135 2(10)	−0.503(23)		69	77	3.1
021, 1*e* - 001, 1*e*	663.928 97(4)	−2.178 39(28)	0.139(4)		94	145	2.3
021, 1*f* - 001, 1*f*	663.928 89(6)	−2.098 53(31)	−0.179 7(32)		101	164	3.2
020, 0*e* - 000	664.618 970(22)	−2.497 16(10)	0.429 3(8)		118	229	1.8
030, 1*e* - 010, 1*e*	681.045 36(4)	−1.893 24(25)	0.343(3)		93	154	2.4
030, 1*f* - 010, 1*f*	681.045 28(4)	−2.154 67(24)	0.377 9(26)		102	167	2.6
040, 2*ef* - 020, 2*ef*	694.983 31(5)	−1.740 3(7)	0.231(16)		67	110	2.5
FCC^{37}Cl:							
001, 1*ef* - 000	209.886 21(12)	−1.699 7(8)	0.136(10)	5.638(7)	89	103	4.3
010, 1*e* - 000	320.998 4(3)	−1.814 2(9)	−0.14fix	3.60fix	69	24	6.2
002, 0*e* - 000	415.444 99(14)	−3.350 8(12)	−1.065(22)		75	72	4.2
011, 0*e* - 000	530.640 28(8)	−3.464 0(8)	−2.204(14)		81	126	4.4
021, 1*e* - 001, 1*e*	661.442 01(14)	−2.121 3(14)	−0.198(27)		71	70	4.1
021, 1*f* - 001, 1*f*	661.442 96(11)	−1.618 2(12)	−0.497(26)		70	77	4.1
020, 0*e* - 000	662.929 433(32)	−2.584 88(19)	0.349 0(21)		102	168	2.2
030, 1*e* - 010, 1*e*	678.905 84(10)	−1.979 3(8)	0.299(13)		79	87	3.4
030, 1*f* - 010, 1*f*	678.905 76(15)	−2.238 8(17)	0.27(4)		63	66	3.5

[a] Dimensionless. [b] H_v 1.256(12)$\times 10^{-13}$ cm^{-1}.

Ground state parameters of FCCCl have been determined both by millimeterwave (MMW) spectroscopy [2] and from 791 ^{35}Cl (251, ^{37}Cl) ground state combination differences (GSCD) obtained from different rovibrational bands [6]. We have now enlarged the body of GSCD and improved the parameters, Table 2. Both sets of ground state parameters are consistent and are not too different in quality, Table 2, but differently composed. Finally we have obtained "ultimate" parameters by a merge of both data sets, with a weight of 50000 attributed to the ca. 250 times more precise rotational data. The "best" ground state constants are reported in column 3 of Table 2. In the fits of rovibrational lines the ground state parameters were held fixed at these values.

Table 3 collects the results of the band fits for FCC^{35}Cl and FCC^{37}Cl, respectively. The rotational parameters of the $v_5 = 1$ excited state have been determined previously by MMW spectroscopy with $J''_{\text{max}} = 18$ [15], and from 410 lower state combination differences (LSCD) formed from P($J + 1$) and R($J - 1$) lines up to $J' = 101$ (^{35}Cl) of hot bands with ν_5 as lower state [6], Table 4. We now have enlarged the quantity of data and also obtained LSCD for the $v_5 = 1$ state of FCC^{37}Cl. Moreover $v_5 = 1$ parameters have been obtained directly from the analysis

Table 4. Parameters (cm^{-1}) of the v_5 = 1 and v_4 = 1 States of FCC^{35}Cl/FCC^{37}Cl.

Ground State	FCC^{35}Cl/FCC^{37}Cl
$B_0 \times 10^2$	7.421 280 37/7.243 894 2
$D_0 \times 10^9$	4.813 1/4.602 4

	MMW[a]	LSCD[a]	Merged data	IR	*ab initio*; ^{35}Cl
$v_5 = 1$:					
ν_{BC}				210.502 45(5)/209.886 21(12)	212.61
$(B_0 - B_5) \times 10^4$	−1.741 8(8)/−1.700 1(11)	−1.739(2)/−1.656(19)	−1.741 6(6)/−1.700 9(9)	−1.740 3(4)/−1.699 7(8)	−1.713
$D_5 \times 10^9$	4.99(9)/4.61(12)	4.93(1)/4.03(17)	4.954(6)/4.74(8)	4.940(4)/4.738(10)	
$q_5 \times 10^5$	5.950(2)/5.689(2)	5.89(1)/5.90(7)	5.946(3)/5.689(4)	5.915 8(11)/5.638(6)	5.519[b]
$\sigma(\text{Fit}) \times 10^4$	0.011/0.010	2.4/4.0	0.11/0.05	3.3/4.3	
No. of data[c]	12/8	524/36	536/44	220/103	
J'_{max}[c]	19/19	101/66	101/66	94/89	
$v_4 = 1$:					
ν_{BC}				321.270 24(6)/320.998 4(3)	321.42
$(B_0 - B_4) \times 10^4$		−1.970(4)/−1.933(18)		−1.968 3(6)/−1.99(8)	−1.985
$D_4 \times 10^9$		4.96(2)/5.02(22)		4.960(7)/4.74fix	
$q_4 \times 10^4$		3.67(2)/3.60(7)		3.713 8(16)/3.60fix	3.583[b]
$\sigma(\text{Fit}) \times 10^4$		2.7/3.7		3.5/6.3	
No. of data[c]		212/45		183/24	
J'_{max}[c]		97/59		82/69	

[a] Data for FCC^{35}Cl from [6]. [b] q_e. [c] Dimensionless.

of the ν_5 bands, Table 4, column 4. In column 3 we also quote the v_5 = 1 parameters which follow from a merge of MMW data weighted 50000 and unit-weighted LSCD.

We note consistency of rotational parameters coming from the different sources. In particular with regard to D the IR data are superior to any of the other results. The *ab initio* results are included for comparison.

The v_4 = 1 state has not yet been studied by rotational spectroscopy but we have at hand LSCD data for both isotopic species up to J' = 97/59. In addition, there are IR data for ^{35}Cl with $J' \leq 82$ and for ^{37}Cl with $J' \leq 69$ although only for the e sublevel, Table 4. As far as any comparison is possible all results agree within one standard deviation.

For the 010, 1*ef* - 000, 001, 1*ef* - 000 and 002, 0*e* - 001, 1*ef* bands both the *e* - *e* and *e* - *f* (*f* - *e*) components have been fitted together while in all other cases *e* - *e* and *f* - *f* transitions have been treated separately. Since doublets of the 040, 2*ef* - 020, 2*ef* hot band were not resolved, the parameters appearing in Table 3 refer to both subbands. B_v values are related to B_v^e and B_v^f values according to (5).

In the numerical fit of the different cold and hot bands we have constrained the lower state parameters to those reported in Table 2, column 3 (ground state, best fit) for the cold bands and in the case of hot bands those in Table 4, column 3 (merged data) for v_5 = 1 as lower state and columns 4 (^{35}Cl) and 2 (^{37}Cl) for the v_4 = 1 state. The parameters of the 020, 2*ef* state which is the lower state of the 040, 2*ef* - 020, 2*ef* band (only observed for ^{35}Cl) were obtained by LSCD. These 020, 2*ef* parameters, B_v 7.460 238(8) × 10^{-2} cm^{-1}, and D_v 4.92(15) × 10^{-9} cm^{-1}, should be taken with due reservation because of the inability to resolve the *ef* doublets.

The $2\nu_5/\nu_4 + \nu_5/\nu_3/2\nu_4$ Tetrad

This tetrad comprises four Σ-type parallel bands consisting of P and R branches. The $\nu_4 + \nu_5$ and $2\nu_4$ bands which are of weak to medium intensity have been analyzed previously [6], and the $\nu_4 + \nu_5$ band has been illustrated in that study. Figure 3 shows the $2\nu_4$ band, which is overlapped by the intense bending vibration of CO$_2$ present as a contaminant. One reason for showing this band here are the striking features associated with the largely blue-shifted hot bands 030, 1*ef* - 010, 1*ef* (C and C'), for which some assignments are given as well in the lower part of Fig. 3, and 040, 2*ef* - 020, 2*ef* (D).

The ν_3 band near 575 cm^{-1} and the $2\nu_5$ band near 416 cm^{-1} are so weak that only the two cold systems of the ^{35}Cl species and the $2\nu_5$ cold band of the ^{37}Cl species have been detected and analyzed, Table 3.

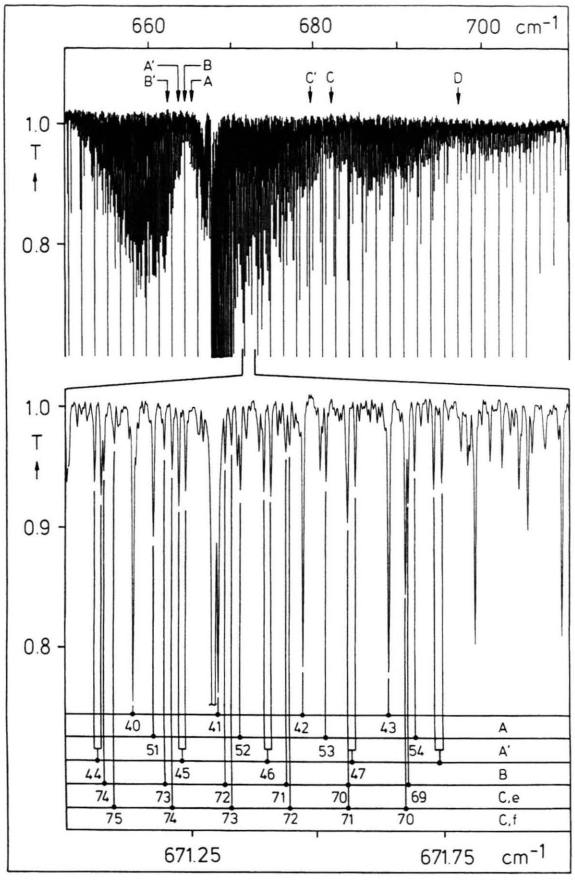

Fig. 3. The $2\nu_4$ band of FCCCl. – *Top:* Survey spectrum. The most prominent lines belong to some CO_2 present in the sample. The denoted band centers belong to the following bands. A, A': $2\nu_4$, $^{35/37}$Cl; B, B': ($2\nu_4 + \nu_5$, $1ef$) – ν_5, $1ef$, $^{35/37}$Cl; C, C': ($3\nu_4 - \nu_4$, $1ef$) – ν_4, $1ef$, $^{35/37}$Cl; D: $4\nu_4$, $2ef$ - $2\nu_4$, $2ef$, ^{35}Cl. – *Bottom:* Detail of the spectrum, with J assignment for R lines (A, A', B) and P lines (C).

The fit to polynomials in $J(J + 1)$ of the four cold bands of FCC^{35}Cl, the three cold bands observed for FCC^{37}Cl, and several hot bands, has been performed, Table 3. Standard deviations between 1.8 and 4.4×10^{-4} cm^{-1} were achieved, which correspond to the quality of the data, residuals being random. The effective spectroscopic parameters obtained by combining lower and upper state parameters are set out in Table 5.

Table 5. Effective excited state parameters of FCCCl (cm^{-1}).

$v_3v_4v_5,\ell$	ν_{BC}	$B_v \times 10^2$	$D_v \times 10^9$	$H_v \times 10^{13}$	$q_v \times 10^5$
FCC^{35}Cl:					
001,1*ef*	210.502 45(5)	7.438 683(5)	4.940(6)		5.915 8(11)
010,1*ef*	321.270 24(6)	7.440 963(7)	4.960(9)		3.713 8(16)
002,0*e*	416.841 33(6)	7.455 613(5)	5.931(8)		
002,2*e*	420.999 15(20)	7.456 163(14)	4.334(18)		
002,2*f*	420.999 82(20)	7.456 109(15)	5.052(10)		
011,0*e*	531.489 51(6)	7.457 194(7)	8.669(19)	1.256(12)	
100	574.274 63(9)	7.422 632(10)	5.316(25)		
020,0*e*	664.618 970(22)	7.446 251 9(18)	4.384(10)		
012,1*e*	741.579 25(10)	7.473 957(9)	4.761(11)		
012,1*f*	741.578 72(10)	7.475 883(9)	5.455(10)		
021,1*e*	874.431 42(9)	7.457 507(8)	4.815(10)		
021,1*f*	874.431 34(10)	7.462 654(8)	5.126(9)		
030,1*ef*	1002.315 55(10)	7.461 200(10)	4.593(10)		6.349(4)
FCC^{37}Cl:					
001,1*ef*	209.886 21(12)	7.260 891(9)	4.738(15)		5.638(7)
010,1*e*	320.998 4(3)	7.262 035 2(20)	4.74fix		
002,0*e*	415.444 99(14)	7.277 402(13)	5.667(26)		
011,0*e*	530.640 28(8)	7.278 535(9)	6.806(19)		
020,0*e*	662.929 433(32)	7.269 743 0(32)	4.253(26)		
021,1*e*	871.328 21(25)	7.279 272(22)	4.94(11)		
021,1*f*	871.329 16(22)	7.279 931(20)	5.24(11)		
030,1*ef*	999.904 2(4)	7.284 311(20)	4.45(4)		6.18(23)

The unusually large ($D'' - D'$) values apparent for the $\Sigma^+ - \Sigma^+$ transitions of $2\nu_5$ and ($\nu_4 + \nu_5$) indicate effects of ℓ-type resonance between the 0*e* and 2*e* levels. The negative signs of the ($D'' - D'$) values suggest that the 2*e* levels of $2\nu_5$ and $\nu_4 + \nu_5$ are *above* the 0*e* ones, that of $2\nu_5$, $\ell = 2e,f$ fortunately being available by means of the $2\nu_5 - \nu_5$ hot band, Tables 3 and 5. These 2*e* levels can be included in the deperturbation of the Σ^+ tetrad provided the B' and D' values of the Δ levels are constrained to extrapolations from ν_4 and ν_5 and moreover the $2\nu_5$, Δ vibrational term value is fixed to that reported in Table 5. On the other hand the 0*e* and 2*e* levels of $\nu_4 + \nu_5$ are so close that the 2*e* band center can be determined from the line shifts due to ℓ-type resonance. To the contrary the 020, 0*e* - 000, 0*e* band was fitted without requiring any extraordinary ($D'' - D'$) value, thus the Σ^+ and Δ vibrational levels should be rather apart.

IV. Interaction Model

When comparing the ($B_0 - B'$) values of the ν_5 and ν_4 bands, Table 4, with those of the overtones $2\nu_5$, $\nu_4 + \nu_5$, and $2\nu_4$ we note that linear v-dependence is reasonably fulfilled for the two former while those of the latter one differ substantially (in 10^{-4} cm^{-1} obs. –2.497/–2.585 vs. calc. –3.94/–3.88 for $^{35/37}$Cl). As was concluded earlier [6], the strong anharmonic resonance between ν_3 and $2\nu_4$, 0*e* dominates the interactions in the 400 - 700 cm^{-1} region, and the previously available data on $\nu_4 + \nu_5$ and $2\nu_4$ have been fitted employing the two cubic interaction constants W_{344} = 37.3 cm^{-1} and W_{345} = 6.8 cm^{-1} as obtained by *ab initio* calculations [6]. The deperturbed wavenumber of

Table 6. Effective, fitted, and predicted rovibrational parameters (cm^{-1}) of $FCC^{35}Cl$.

	Effective	Fitted, deperturbed	Predicted from ν_4 and ν_5	*ab initio*, deperturbed
$2\nu_5$:				
ν_{BC}, Σ^+	416.841 33(6)	424.645 23(5)	421.0^c	429.10
$(B_0 - B_v)\times 10^4, \Sigma^+$	−3.433 2(4)	−3.644 0(3)	−3.48	−3.43
$(D_0 - D_v)\times 10^9, \Sigma^+$	−1.118(5)	−0.25^a	−0.25	
ν_{BC}, Δ		420.999 5^a		
$(B_0 - B_v)\times 10^4, \Delta$		−3.48^a		
$(D_0 - D_v)\times 10^9, \Delta$		−0.25^a		
$W_{55}\times 10^5$		6.053(15)		
$\nu_4 + \nu_5$:				
ν_{BC}, Σ^+	531.489 51(6)	532.048 04(4)	531.8^c	532.36
$(B_0 - B_v)\times 10^4, \Sigma^+$	−3.591 4(6)	−3.639 70(5)	−3.71	−3.70
$(D_0 - D_v)\times 10^9, \Sigma^+$	−3.856(17)	−0.27^a	−0.27	
$H_v\times 10^{13}, \Sigma^+$	1.256(12)			
ν_{BC}, Δ		532.095(4)		
$(B_0 - B_v)\times 10^4, \Delta$		−3.71^a		
$(D_0 - D_v)\times 10^9, \Delta$		−0.27^a		
$W_{45}\times 10^5$		4.797(8)		
ν_3:				
ν_{BC}, Σ^+	574.274 63(9)	587.393 49(10)		587.03
$(B_0 - B_v)\times 10^4, \Sigma^+$	−0.135 2(10)	1.181 8(11)		1.22
$(D_0 - D_v)\times 10^9, \Sigma^+$	−0.503(23)	−0.241(25)		
$2\nu_4$:				
ν_{BC}, Σ^+	664.618 970(22)	643.137 39(5)	642.5^c	649.75
$(B_0 - B_v)\times 10^4, \Sigma^+$	−2.497 16(10)	−3.562 6(3)	−3.94	−3.97
$(D_0 - D_v)\times 10^9, \Sigma^+$	0.429 3(8)	0.105(7)	−0.29	
W_{355}		b		36.3
W_{345}		b		−6.8
W_{344}		b		37.3
W_{4445}		b		−3.8
W_{4555}		b		1.5
W_{4455}		b		8.6
$\sigma\times 10^4$		2.17		

[a] Constrained. [b] Adopted from *ab initio* calculations. [c] Without anharmonicity corrections.

the formerly unobserved ν_3 vibration was estimated from perturbational effects to be 604.5 cm^{-1} [6].

Combined Experimental and Theoretical Analysis

We have now extended the interaction model to three more levels, namely $2\nu_5(\Sigma^+)$, $2\nu_5(\Delta)$ and $\nu_3(\Sigma^+)$. The relevant quartic interaction constants W_{4445}, W_{4455} and W_{4555} [6] are now taken into account as well as the cubic constant W_{355} that has become relevant since ν_3 and $2\nu_5$ have been observed. Of the models conceivable that allow a fit of the 4 Σ^+ + 2 Δ, *e* interacting systems (see e. g. [8]), this model is the most comprehensive and physically meaningful one, although agreement of predictions and observations was also achieved with simpler truncated models [6]. It takes into account all experimental data related to the $v_3 = 1$, $v_4 = 2$, $v_4 = v_5 = 1$ and $v_5 = 2$ states. It constrains "experimentally predictable" parameters, *i. e.*, $(B_0 - B')$ and $(D_0 - D')$ of the doubly excited states, to their extrapolated values and adopts the *ab initio* values for the three cubic and three quartic interaction constants. The results based on altogether 638 observed transitions which were fitted with $\sigma = 2.17\times 10^{-4}$ cm^{-1} are reported in Table 6, column 2 (fitted, deperturbed). A graphical illustration and comparison with effective parameters is displayed in Figure 4.

Although this model only concerns $FCC^{35}Cl$ it should also be applicable to $FCC^{37}Cl$. Regrettably some data related to ν_3 and $2\nu_5$, Δ, are missing which are needed for a successful transfer and application of the present model to this less abundant isotopomer.

In comparison to the effective parameters, Table 6, column 1, the deperturbed band centers and $(B_0 - B_v)$ values of ν_3 and $2\nu_4$, column 2, are much closer to the extrapolation from experiment and the *ab initio* predictions, columns 3 and 4. Moreover, the $(D_0 - D_v)$ values in column 2 are much smaller and hence more meaningful than those in column 1.

With regard to $2\nu_5$ and $\nu_4 + \nu_5$, the band centers and $(B_0 - B_v)$ values do not change dramatically upon anharmonic deperturbation while the $(D_0 - D_v)$ values and H_v values relax to a "meaningful" size when rotational ℓ-type resonance is taken into account. However, this model leads to large shifts for the ν_3 and $2\nu_4$ levels, indicating the dominant influence of the $\nu_3/2\nu_4$ Fermi interaction.

Comparison between Experiment and Theory

The preceding analysis provides deperturbed experimental wavenumbers ν_{BC}, Table 6. It is instructive to compare these values with purely *ab initio* predictions. These can be derived from the MP2/TZ2Pf [6] harmonic wavenumbers (ω_i) and anharmonicity constants (x_{ij}, g_{ij}) given in Table 7. Consistency is essential in such comparisons, i. e. interactions that are handled explicitly in the experimental fit model must be excluded from the perturbational summations used to determine the theoretical anharmonicity constants. Such an explicit treatment has previously been applied for the strong $\nu_1/2\nu_2$ and $\nu_3/2\nu_4$ Fermi resonances (see [6], model 1) and is now extended to several other anharmonic interactions (see Table 6 and Figure 4). The corresponding sets of effective anhar-

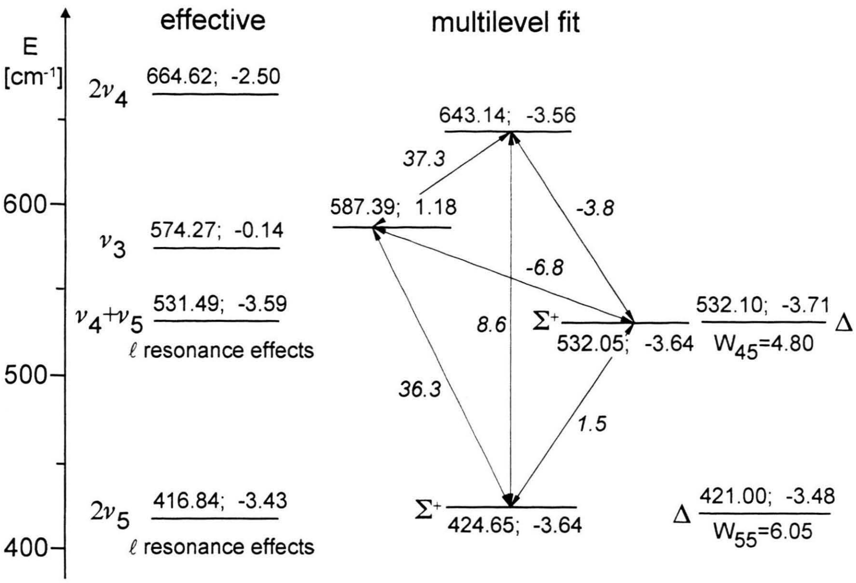

Fig. 4. Graphical display of effective and deperturbed band centers (cm^{-1}), ($B_0 - B_v$) values (10^{-4} cm^{-1}) and ℓ-type interaction constants W_{ij} (10^{-5} cm^{-1}). Anharmonic constants (cm^{-1}) from *ab initio* calculations are given in italics.

Table 7. *Ab initio* anharmonicity constants (cm^{-1}) of FCC^{35}Cl[a].

	$i\ j$	Purely perturbational	Previous model[b]	Present model[c]
x_{ij}	1 1	−10.14		
	1 2	−47.58	−4.05	
	1 3	−2.59		
	1 4	−26.21		
	1 5	−3.61		
	2 2	+6.27	−4.61	
	2 3	+0.99		
	2 4	−1.32		
	2 5	−1.68		
	3 3	−2.02		
	3 4	−22.22	−1.68	−2.64
	3 5	+6.11		−2.82
	4 4	+7.42	+2.28	+2.28
	4 5	−2.11		−1.63
	5 5	−0.98		+1.02
g_{ij}	4 4	−6.24	−1.11	−1.11
	4 5	+0.65		+0.18
	5 5	+1.14		−0.85

[a] MP2/TZ2Pf values, computational details see [6]; harmonic wavenumbers ω_i (cm^{-1}) for i = 1 - 5: 2387.60, 1236.38, 597.33, 332.47, 216.17. [b] [6]: Effective constants without contributions from $\nu_1/2\nu_2$ and $\nu_3/2\nu_4$. [c] This work: Effective constants without contributions from $\nu_3/2\nu_4$, $\nu_3/\nu_4 + \nu_5$, and $\nu_3/2\nu_5$; used to compute the deperturbed wavenumbers in Table 8.

monicity constants are listed in the last two columns of Table 7.

Table 8. Comparison between experimental and theoretical wavenumbers (cm^{-1}).

	— Experiment[a] —		— Theory[b] —	
	effective	deperturbed	deperturbed	anharmonic
Σ^+ states:				
$2\nu_5$	416.84	424.65	429.10	421.09
$\nu_4 + \nu_5$	531.49	532.05	532.36	531.80
ν_3	574.27	587.39	587.03	575.66
$2\nu_4$	664.62	643.14	649.75	669.69
Δ states:				
$2\nu_5$	421.00			425.69
$\nu_4 + \nu_5$	532.08			532.71
$2\nu_4$				645.32

[a] See Tables 5 and 6. [b] Based on the data in Table 7. See text for details.

Experimental and theoretical wavenumbers in the range between 400 - 700 cm^{-1} are compared in Table 8. The deperturbed theoretical wavenumbers for the Σ^+ transitions in the $2\nu_5/\nu_4 + \nu_5/\nu_3/2\nu_4$ tetrad are in excellent agreement with their experimentally derived counterparts, with deviations between 0 and 6 cm^{-1}. Diagonalization of the corresponding 4×4 matrix (with the *ab initio* interaction constants from Table 6) yields the anharmonic theoretical wavenumbers for the tetrad which again agree very well with the observed effective values (see Table 8). In the case of the Δ transitions ($2\nu_5$, $\nu_4 + \nu_5$, $2\nu_4$), there is no need for deperturbation since there are no longer any particularly strong anharmonic interactions (due to the absence of ν_3). A standard perturbational approach provides *ab initio* predictions for the Δ states which are close to the available experimental data for

$2\nu_5$ and $\nu_4 + \nu_5$; note, in particular, that the Δ/Σ^+ splittings are reproduced well (see Table 8). Based on these observations and taking the deviations for $2\nu_4$ (Σ^+) into account, we expect the unknown Δ state of $2\nu_4$ to lie at 640 cm^{-1}.

V. Conclusions

The present study has revealed extended anharmonic interactions between Σ^+-type levels in the 400 - 700 cm^{-1} region. A detailed understanding of these interactions has been achieved through a combined experimental and theoretical approach. It is to be expected that such interactions will also affect Σ^+-type overtone levels at twice this energy, which is that of the CF stretching vibration. The results of the present study will be helpful to better understand the complex ν_2 region near 1205 cm^{-1} in terms of "perturbed perturbers".

Acknowledgements

This work was supported by the Deutsche Forschungsgemeinschaft, the Fonds der Chemie, and the Schweizerischer Nationalfonds.

[1] H. Bürger, W. Schneider, S. Sommer, W. Thiel, and H. Willner, J. Chem. Phys. **95**, 5660 (1991).

[2] A. Guarnieri and M. Andolfatto, Z. Naturforsch. **36a**, 899 (1981).

[3] M. Andolfatto, B. Kleibömer, and A. Guarnieri, Z. Naturforsch. **37a**, 1449 (1982).

[4] T. Hirao, T. Okabayashi, and M. Tanimoto, J. Mol. Spectrosc. **162**, 358 (1993).

[5] J. Breidung, T. Hansen, and W. Thiel, J. Mol. Spectrosc. **179**, 73 (1996).

[6] J. Breidung, H. Bürger, M. Senzlober, and W. Thiel, Ber. Bunsenges. Phys. Chem. **99**, 282 (1995).

[7] J. Breidung, H. Bürger, D. McNaughton, M. Senzlober, and W. Thiel, Spectrochim. Acta **55A**, 695 (1999).

[8] H. Bürger and W. Thiel in: Vibration-Rotational Spectroscopy and Molecular Dynamics. Advances in Quantum Chemical and Spectroscopical Studies of Molecular Structures and Dynamics, (D. Papoušek, Ed.), pp. 56-115, World Scientific, Singapore 1997.

[9] S. Y. Delavarenne and H. G. Viehe, Chem. Ber. **103**, 1198 (1970).

[10] A. Runge and W. W. Sander, Tetrahedron Lett. **31**, 5453 (1990).

[11] M. Birk, M. Winnewissser, and E. A. Cohen, J. Mol. Spectrosc. **136**, 402 (1985).

[12] G. Guelachvili and K. Narahari Rao, Handbook of Infrared Standards, Academic Press, San Diego 1986.

[13] B. P. Winnewisser, J. Reinstädtler, K. M. T. Yamada, and J. Behrend, J. Mol. Spectrosc. **136**, 12 (1989).

[14] C. Betrencourt-Stirneman, G. Graner, D. E. Jennings, and W. E. Blass, J. Mol. Spectrosc. **69**, 179 (1978).

[15] T. Okabayashi and M. Tanimoto, J. Mol. Spectrosc. **154**, 201 (1992).

[16] K. Yamada, J. Mol. Spectrosc. **79**, 323 (1980).